Calculation of NMR Chemical Shifts and Spin−Spin Coupling Constants in the Monosaccharide Methyl-β-D-xylopyranoside Using a Density Functional Theory Approach†

M. Hricovíni,‡ O. L. Malkina,§ F. Bízik,⊥ L. Turi Nagy,|| and V. G. Malkin*,||

Institute of Chemistry, Computing Center, Institute of Virology, and Institute of Inorganic Chemistry, Slovak Academy of Sciences, SK-84236 Bratislava, Slovakia

Received: June 25, 1997; In Final Form: September 24, 1997⊗

Density functional theory based approaches were used to calculate chemical shieldings and spin−spin coupling constants in a monosaccharide, methyl-β-D-xylopyranoside. Excellent agreement was found between the computed and experimental data for this monosaccharide both in solution and in solid state. The effect of torsion around the C1−O1 bond showed that chemical shifts of the anomeric proton, both ring and O1 oxygens as well as C1, C2, and the methyl carbons, strongly depend on the dihedral angle. Similarly, both one-bond and three-bond proton−carbon coupling constants among anomeric proton and anomeric and methyl carbons [($^1J_{C1-H1}$) and ($^3J_{C(Me)-H1}$), respectively] showed a dependence on the torsion angle Φ.

1. Introduction

Relations between NMR parameters, chemical shifts, and spin−spin coupling constants and molecular structure are of primary importance for determination of the structure, conformation, and dynamics of chemical compounds both in solution and in solid state. Since experimental relations rely mostly on empirical data without detailed understanding of their physical origin, there is a need for more fundamental studies based on theoretical analysis of chemical shielding tensors and coupling constants. Moreover, in principle, theoretical calculations might provide NMR parameters−structure relations where experimental data are limited.

Recent advances in theory and computational approaches allow one to compute these NMR parameters with acceptable accuracy in relatively simple chemical systems.[1−8] Taking into account that NMR chemical shift and spin−spin coupling constants are mostly determined by the local structure, these simple chemical systems can provide reliable models for larger molecules. However, the combination of reliability and efficiency of a computational method remains the most important characteristic of the approach. From this point of view the most promising present methods are based on density functional theory (DFT).[1−3] Sum-over-states density functional perturbation theory (SOS-DFPT)[2,3] for calculation of shielding tensors and the DFT based approach of Malkin et al.[1,3,7] for calculation of coupling constants have been successfully applied for various compounds with very good agreement between theory and experiment.[1−3,7−10]

Carbohydrates belong to chemical structures thoroughly investigated due to their various important biological activities. In this paper, an analysis of relations between the structure and NMR shielding tensor and coupling constant in a monosaccharide, methyl-β-D-xylopyranoside (**I**) using DFT based methods is presented. The computed NMR parameters are compared with experimental values, and their dependence on structure is discussed in terms of anomeric and γ-gauche effects.

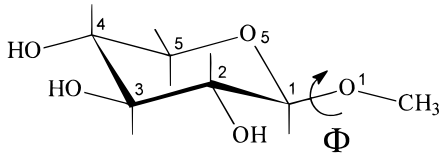

2. Methods

The DFT calculations have been carried out using a modified version of the deMon-KS program[11,12] augmented by the deMon-NMR code.[1−3] All calculated couplings have been obtained with Perdew and Wang exchange[13] with the Perdew correlation functional.[14] For chemical shift calculations a new Perdew and Wang exchange-correlation functional (PW91)[15] was used. The geometry was optimized with Becke exchange[16] and Perdew correlation functionals.[14] See refs 1−3 for further computational details. For calculations of couplings and chemical shifts the basis set BIII of Kutzelnigg et al.[17] (also called IGLO-III in some other publications) was used. Besides the basis set BIII, we also used a smaller TZVP basis[18] for the optimization of the structure. FINE grid with 32 (for the optimization of the structure, chemical shift calculations, and the calculation, of the PSO and DSO contributions to spin−spin couplings) and 64 (for the FC term calculations) points of radial quadrature[19] was employed. The use of the *individual gauge for localized orbitals* (IGLO)[17] for shielding tensor ($\boldsymbol{\sigma}$) calculations allows us to decompose the principal components of σ_{ii} in terms of contributions from localized molecular orbitals (LMO). We will denote the contribution from a particular LMO to σ_{ii} as σ_{ii} (LMO).

Since the optimization of the structure is the bottleneck of the whole computational procedure, a cheaper computational method for geometry optimization (MM2 method within the MacroModel, V5.0[20]) was also used. We will refer to the geometries optimized with MM2 and DFT method as MM2 and DFT geometries. In addition, to study the dependence of NMR parameters on the dihedral angle ϕ [$\phi = \phi$(H1−C1−O1−C_{Me})], the geometry was fully optimized (at the DFT level) except for ϕ, which was kept fixed for different conformations (ϕ = 0, 30, 60, ..., 330°).

NMR experiments were carried out on a Bruker AM300 and AMX500 spectrometers in D_2O at 303 K. The experimental

* Corresponding author: e-mail malkin@savba.sk; Fax (421-7) 373-541; phone (421-7) 378-2923.

† Presented at the 4th International Satellite Meeting on the Conformational Analysis of Carbohydrates, July 17−20, 1996, La Thuile, Italy.

‡ Institute of Chemistry.
§ Computing Center.
⊥ Institute of Virology.
|| Institute of Inorganic Chemistry.

⊗ Abstract published in *Advance ACS Abstracts,* November 15, 1997.

S1089-5639(97)02071-9 CCC: $14.00

TABLE 1: SOS-DFPT Computed Chemical Shieldings (at Equilibrium Geometry Calculated by DFT with TZVP Basis) and Experimental Chemical Shifts for Methyl-β-D-xylopyranoside (All Values in ppm)

	SOS-DFPT					experiment		
	σ_{11}	σ_{22}	σ_{33}	σ_{iso}	σ_{iso}[a]	solution	solid state[b]	solid state[b]
C-1	47.87	69.96	82.15	66.66	105.23	105.10	104.2	105.1
C-2	81.61	97.36	114.21	97.85	74.04	74.11	72.2	73.4
C-3	81.96	91.35	111.77	95.03	76.86	76.86	78.2	79.1
C-4	84.95	90.77	132.23	102.65	69.24	70.33	69.5	70.4
C-5	74.39	94.61	154.47	107.82	64.07	66.26	66.9	67.6
OMe	83.44	99.18	178.78	120.46	51.43	58.34	57.3	58.3

[a] Referenced to experimental value of C-3 (in solution). [b] References 23 and 24.

values of proton−proton couplings were based on first-order analysis of proton spectra; one-bond proton−carbon coupling constants were measured from proton−carbon coupled spectra. Long-range C−H coupling constants were determined either from two-dimensional carbon-detected semiselective INEPT[21] or from selective one-dimensional proton-detected experiment.[22] The digital resolution of one-dimensional spectra was 0.1 Hz. In the two-dimensional INEPT experiment, selected traces in the F2 domain of the 2D matrix were zero-filled to give a digital resolution of 0.15 Hz. The values of chemical shifts are relative to external TSP ($\delta_{TSP} = 0$ ppm).

3. Results and Discussion

The principal components of chemical shifts tensors (σ_{ii}) and the isotropic values obtained by the SOS DFPT method for DFT geometries together with the experimental values (liquid and solid states[23,24]) for methyl-β-D-xylopyranoside are given in Table 1. The values of the principal components of individual carbons vary considerably, reflecting rather different structural features among the carbons, mainly between the anomeric (C1) and methyl carbon (C_{Me}). The most similar principal components are found for primary alcohol carbons, C2, C3, and C4. This relative consistency is due to the structural similarity of carbons where each is bearing an OH group and is bound to a similar type of carbon. However, C4 still has rather distinguished shieldings since the tensor can be approximated with axial symmetry ($\sigma_{11} \approx \sigma_{22}$). A similar approximation can also be done for methyl carbon. Further recognition of similarities among the computed shielding constants and its relation to structure is not obvious.

To transfer the calculated shieldings to chemical shifts, the value of the chemical shift for the C3 ring carbon was fixed equal to the experimental value for this carbon, $\delta_{C3} = 76.86$ ppm. The comparison of computed relative isotropic shifts with the experimental values indicates very good agreement between the data sets−within 1 ppm for methine carbons and about 2 ppm for methylene C5. The largest deviation is observed for OMe carbon (about 7 ppm). However, this deviation for OMe carbon is quite expected because of the flexibility of the fragment due to rotation around the C1−O1 bond. Since the dependencies of NMR parameters on such rotations are of general interest, the dependence of the OMe carbon chemical shift and other NMR parameters on the torsion angle ϕ has been studied (see below). Another possible reason for the discrepancy between the calculated and experimental NMR parameters is the neglect of solvent effects during both the calculations of chemical shifts (direct effect) and the geometry optimization (indirect effect). Due to the flexibility of the OMe group, the chemical shift of methyl carbon might be at first affected by solvent effects.

TABLE 2: Computed Coupling Constants (in Hz) for MM2 (Column 1) and DFT (Column 2) Geometries; Experimental Values for Methyl-β-D-xylopyranoside Are Given in the Last Column

	MM2	DFT	expt
$^1J_{C1-H1}$	156.7	151.20	161.7
$^1J_{C2-H2}$	145.1	140.06	146.4
$^1J_{C5-H5eq}$	143.4	144.36	150.2
$^1J_{C5-H5ax}$		132.50	140.0
$^3J_{H1-COme}$	3.07	4.19	4.5
$^3J_{H1-C3}$	0.95	1.13	1.0
$^3J_{H1-C5}$	1.25	1.15	1.5
$^3J_{H2-C4}$	0.95	1.01	1.4
$^3J_{H5eq-C1}$	11.64	11.59	10.2
$^3J_{H5eq-C3}$	9.47	9.58	9.5
$^3J_{H5ax-C1}$		3.14	3.2
$^3J_{H5ax-C3}$		2.92	2.6
$^2J_{H1-C2}$	2.95	2.04	2.3
$^2J_{H2-C1}$	−2.51	−3.33	3.2
$^2J_{H2-C3}$	−2.91	−3.40	3.3
$^2J_{H5eq-C4}$	−2.38	−2.48	3.5
$^2J_{H5ax-C4}$		−1.44	2.1
$^3J_{H1-H2}$	6.57	6.91	7.8
$^3J_{H2-H3}$	8.06	8.43	9.3
$^3J_{H4-H5eq}$	4.93	4.92	5.4
$^3J_{H4-H5ax}$		9.74	10.5
$^2J_{H5ax-H5eq}$	−10.41	−9.25	−11.5

The computed (for MM2 and DFT geometries) and the experimental values of proton−proton and proton−carbon coupling constants are listed in Table 2. The calculated one-bond proton−carbon couplings are 6−10 Hz smaller than the experimental values. (The deviation is about 5% of the experimental values.) The error for the anomeric center ($\Delta^1J_{C1-H1} = 10.5$ Hz) is the largest one observed for couplings computed at DFT geometries. In previous studies[1,3,7] it was shown that one-bond proton−carbon couplings usually deviate from experimental data in both directions. Therefore, the systematic underestimation of one-bond proton−carbon couplings in the present calculations likely reflects some inaccuracy in the geometries and/or neglect of solvation effects. The influence of the structure used on the calculated spin−spin couplings is well shown by comparison of the calculated couplings for the MM2 and DFT geometries. Different ways to include solvation effects into the calculations will be the subject of our future studies.

However, even at the present level of theory, the trend for the one-bond couplings is well reproduced. For example, $^1J_{C5-H5ax}$ and $^1J_{C5-H5eq}$ differ about 11 Hz from each other, $^1J_{C5-H5eq}$ being smaller, which is in good agreement with experiment. This difference between $^1J_{C5-H5ax}$ and $^1J_{C5-H5eq}$ is due to orientation of ring oxygen lone pairs. The overlap between the occupied lone-pair molecular orbital (MO) and the MO of the C−H bond is stronger in the gauche position. Since the magnitudes of $^1J_{C-H}$ also depend on changes in geometry through the change of s-character of C−H bond and s-orbital densities at the carbon nucleus, $^1J_{C-H}$ for equatorially oriented C−H bond is larger than that for the axial one. This dependence has been previously observed experimentally in carbohydrates[25] and has been used for determination of the configuration at the anomeric center. Therefore, the present computed values of $^1J_{C-H}$ agree with the experimental evidence.

The agreement between theoretical and experimental long-range proton−carbon coupling constants is excellent for practically all couplings (Table 2). It should be noted in this respect that the sign of experimental couplings has not been determined. The computed geminal and vicinal proton−proton couplings are also in good agreement with experiment though their absolute values are somewhat smaller.

TABLE 3: Energy (in au) and Selected Geometrical Parameters (Distances in Å) for Different Conformers on the C1−O1 Linkage in Methyl-β-D-xylopyranoside

ϕ, deg	energy	C1−O1	C1−O5	C1−H1	O5−C1−O1	C2−C1−O1	C1−O1− C_{Me}
0	−612.162 097 06	1.411	1.431	1.122	107.93	108.80	114.04
30	−612.166 758 08	1.401	1.442	1.123	108.44	108.24	113.93
60	−612.167 275 21	1.402	1.434	1.125	109.76	107.04	113.87
90	−612.162 963 08	1.414	1.423	1.126	110.95	106.31	116.26
120	−612.159 394 10	1.423	1.423	1.122	110.99	108.37	118.00
150	−612.161 464 07	1.416	1.430	1.118	110.42	111.36	116.50
180	−612.162 159 47	1.410	1.432	1.117	115.04	113.73	116.57
210	−612.157 743 85	1.408	1.434	1.119	107.09	116.15	117.87
240	−612.151 623 10	1.414	1.434	1.122	104.05	118.14	120.93
270	−612.152 332 18	1.419	1.429	1.124	101.76	117.16	118.90
300	−612.155 261 88	1.417	1.424	1.125	102.16	115.66	116.23
330	−612.158 770 37	1.412	1.431	1.124	104.98	112.93	114.11

The largest contribution to all considered coupling constants is due to the Fermi contact term (FC). The sum of diamagnetic (DSO) and paramagnetic (PSO) spin−orbital contributions to ^1J, ^2J, and ^3J is equal to or less than 1% of the total value. For example, the FC term in $^1J_{C1-H1}$ is 150.67 Hz, the DSO term is 1.61 Hz, and PSO is −1.08 Hz (the total calculated value is 151.20 Hz versus the experimental 161.7 Hz) for the DFT geometry. However, for couplings through more than three bonds, ^4J and ^5J, the relative contributions of DSO and PSO are considerably larger. For example, the FC contribution to $^4J_{H1-H3}$ is −0.05 Hz, the PSO contribution is −2.31 Hz, and the DSO contribution is 2.37 Hz.

If a molecule has a few low-lying conformers, a Boltzmann averaging of the NMR parameters over them might be important.[26] In our case the energy difference is quite large (Table 3), and therefore one should not expect that such averaging will change the results significantly. In fact, the values of chemical shieldings and coupling constants were computed from Boltzmann average from low-energy conformers in a wide range of temperatures (between 100 and 500 K), and the averaged values were comparable with those obtained from the single minimum (within 1%).

3.1. Effect of Torsion on Chemical Shifts. There is experimental evidence that chemical shift values of carbons at the glycosidic linkage depend on the dihedral angles ϕ and ψ in oligo- and polysaccharides. This effect was observed in both α- and β-linked saccharides and discussed in terms of anomeric and exo-anomeric as well as γ-gauche effects.[27−31] The difference of about 2 ppm in the C1 chemical shift was observed in solid-state spectra of β-cellobiose and methyl-β-cellobioside methanolate: δ_{C1} was 104.9 ppm in β-cellobiose (where the torsion angle ϕ is 44°), and the corresponding shift value in methyl-β-cellobioside was 106.5 ppm ($\phi \sim 29°$). Chemical shift values of C-1 and C-4 carbons in chitin and β-1−4 and β-1−3 glucans have also been suggested as probes for conformational changes of the glycosidic linkage.[27] A related recent ab initio study described changes of carbon chemical shieldings, within limited range of dihedral angles, in an acyclic model compound.[32] Comprehensive studies of torsion effects on carbon shieldings in hydrocarbons and peptide model compounds were carried out with ab initio methods.[33,34]

The use of a theoretical approach (DFT in particular) presents a unique opportunity to study the dependencies of NMR parameters (both chemical shifts and coupling constants) on the dihedral angles for the whole range of these angles. Such studies not only give insight into structure−NMR parameters relations but also can be used for averaging of computed values (using Boltzmann statistics) in the case of flat potential surfaces and/or many low-lying conformers.[35] Also, these "Karplus-type" relations might be directly used for NMR structure determination of more complicated species for which methyl-β-D-xylopyranoside is a suitable model.

With this in mind we performed calculations of the NMR parameters for a series of conformers of methyl-β-D-xylopyranoside. We started with a slightly idealized equilibrium structure (the dihedral angle ϕ was chosen to be equal to 60° instead of the optimized angle of 58.1°), and then we changed the angle with the step of 30° in the interval of 360°. The resulting structures were reoptimized with a fixed value of the dihedral angle ϕ. At last, the chemical shifts and coupling constants were calculated for these relaxed structures. Energies and the selected geometrical parameters are given in Table 3. The observed variations of the bond lengths and bond angles are known to be a consequence of electrostatic and stereoelectronic effects.[36] C1−O1 bond lengths have been found to be shorter, on average, by about 0.2 Å than those of C1−O5; however, the difference depends considerably on the conformation on the linkage. The difference in magnitudes of bond angles for different conformers is also pronounced with the largest variations for O5−C1−O1 angle (up to 14°). The glycosidic bond angle has varied from 113.87° (the lowest energy conformer) to 120.93°.

The dihedral angle dependence of the principal components of the calculated shielding tensors (σ_{ii}) and isotropic shieldings (σ_{iso}) for selected atoms is given in Table 4. For some atoms, the shieldings vary considerably. For example, σ_{iso} for C2 changes from 105.22 ppm for the antiperiplanar position of OMe group ($\phi = 180°$) to 93.42 ppm for the gauche conformation ($\phi = 60°$). Similar dependencies are observed also for C_{Me} and C1 carbons though the dependence of C1 is less pronounced. Considerably large differences are also among the individual components of the shielding tensors. For C2 carbon, σ_{11} and σ_{33} change within ∼17 and ∼24 ppm for syn- and antiperiplanar positions, respectively, whereas σ_{22} is constant. The same trend is observed for C_{Me} with almost constant value of σ_{33}. Analysis of the above-mentioned "constant" σ_{ii} components revealed that they are oriented along the chemical bonds C_{Me}−O1 and C1−C2, respectively. This reflects the spatial dependence of separate contributions of LMO's to the σ individual principal components. For example, the contribution of the C_{Me}−O1 bond to OMe carbon shielding is constant for all values whereas the methyl group C−H bonds contributions to σ_{ii} components vary up to ∼50 ppm as a function of ϕ. The overall resulting effect is that σ_{33} (which is collinear with the C_{Me}−O1 bond) is nearly constant. Similar observations were found for the C-2 carbon where σ_{22} is along the C1−C2 bond.

The pronounced dependence of σ_{ii} on the dihedral angle is also found for anomeric carbon. In this case, however, the effect of torsion is not as strong as for previously mentioned nuclei, and σ_{iso} varies within ∼7 ppm (see Figure 1). Inspection of the most important LMO contributions to the principal components shows (Table 5) considerable dependencies of σ_{ii}(LMO) on the dihedral angle as well as their partial mutual compensation. For example, the variations of LMO contributions of the

TABLE 4: Effect of Torsion of ϕ Angle upon the Principal Components of Chemical Shielding Tensors (in ppm) for Selected Atoms as Obtained by the SOS-DFPT Method

	C_{Me}				O-5				C-2			
ϕ, deg	σ_{11}	σ_{22}	σ_{33}	σ_{iso}	σ_{11}	σ_{22}	σ_{33}	σ_{iso}	σ_{11}	σ_{22}	σ_{33}	σ_{iso}
0	79.37	86.81	178.56	114.92	184.46	239.93	262.79	229.06	78.87	98.63	113.82	97.10
30	75.94	93.45	179.61	116.33	184.78	225.96	273.55	228.10	82.16	98.10	116.23	98.83
60	83.44	99.18	178.78	120.46	198.82	224.33	270.95	231.37	81.61	97.74	114.21	97.85
90	93.25	102.57	176.45	124.09	213.63	241.06	262.03	238.90	81.48	97.22	107.72	95.64
120	97.02	104.50	176.28	125.93	210.14	244.88	276.49	243.83	83.85	98.31	109.59	97.25
150	99.19	105.39	177.47	127.35	211.88	238.17	263.26	237.77	86.01	97.75	126.83	103.53
180	99.05	104.83	178.60	127.50	195.22	230.01	277.59	234.27	83.64	96.12	135.90	105.22
210	95.57	102.92	174.25	124.25	180.35	236.81	278.27	231.81	80.11	96.54	127.46	101.37
240	96.24	101.45	177.67	125.12	174.22	238.78	262.61	225.20	75.76	98.31	126.69	100.26
270	95.72	101.45	173.34	123.50	179.94	235.58	263.82	226.45	73.50	99.11	119.43	97.35
300	90.02	97.44	171.44	119.63	184.55	234.26	267.85	228.89	69.15	99.64	111.48	93.42
330	84.51	89.53	177.33	117.12	180.92	237.33	258.32	225.52	69.83	99.60	111.64	93.69

	H-1				C-1				O-1			
ϕ, deg	σ_{11}	σ_{22}	σ_{33}	σ_{iso}	σ_{11}	σ_{22}	σ_{33}	σ_{iso}	σ_{11}	σ_{22}	σ_{33}	σ_{iso}
0	25.06	26.25	29.26	26.86	40.55	65.67	80.96	62.39	195.09	249.59	326.59	257.09
30	25.36	26.54	28.53	26.81	40.57	67.17	78.59	62.11	185.40	244.81	306.70	245.64
60	25.05	27.38	27.87	26.76	47.87	69.96	82.15	66.66	189.07	245.14	296.85	243.69
90	24.08	27.41	28.01	26.50	54.25	68.76	86.14	69.72	210.21	242.57	324.32	259.03
120	23.39	27.47	28.11	26.32	55.82	67.75	85.05	69.54	208.47	269.79	347.61	275.29
150	23.64	27.34	28.16	26.38	51.26	70.47	84.79	68.84	221.99	263.01	329.50	271.50
180	23.90	27.45	28.04	26.46	46.55	71.44	86.65	68.21	217.40	263.82	301.17	260.80
210	23.70	27.58	27.94	26.41	45.86	70.49	88.10	68.15	202.31	259.19	312.19	257.90
240	23.22	27.35	28.03	26.20	47.68	68.99	86.93	67.87	174.77	274.24	327.15	258.90
270	23.58	27.07	28.15	26.26	50.65	65.57	86.78	67.67	180.00	255.75	326.96	254.24
300	24.43	26.95	28.22	26.53	47.64	63.82	85.32	65.59	201.14	229.77	313.66	248.19
330	24.95	26.44	28.82	26.74	43.69	66.14	85.12	64.99	189.99	252.29	317.96	253.41

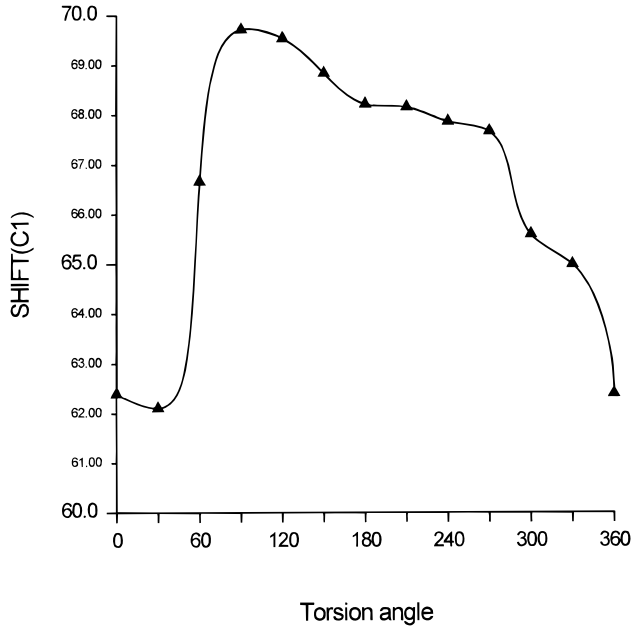

Figure 1. Dependence of the anomeric carbon (C1) shieldings (in ppm) in methyl-β-D-xylopyranoside upon the dihedral angle ϕ (deg) as obtained by the SOS-DFPT method.

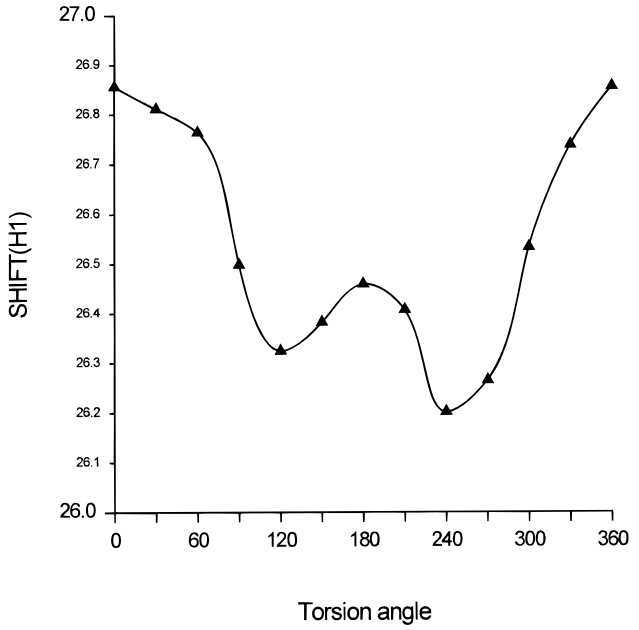

Figure 2. Dependence of the anomeric proton (H1) shieldings (in ppm) in methyl-β-D-xylopyranoside upon the dihedral angle ϕ (deg) as obtained by the SOS-DFPT method.

C1−H1 bond to σ_{11} are as large as ∼40 ppm with the positive σ_{11}(C1−H1) values for conformations close to the anti position. For the same conformations, σ_{22}(C1−H1) show the lowest values (with minimum of −51.9 ppm). This compensation results in relatively constant chemical shift values of C1 within the interval of 90°−270°. However, the values of σ_{iso} vary considerably (up to 6−7 ppm) for conformations with the dihedral angle between 0° and 90° (see Figure 1), which is in agreement with experimental observations.[27−30] If refined sufficiently, this dependence might be used as an additional parameter for estimation of conformation on the glycosidic linkage.

In contrast to the C1 chemical shifts, where the higher shielding values are found for dihedral angles between 90° and 270°, σ_{iso} for H1 is in this interval lower (less shielded) by about 0.6 ppm (Table 4, Figure 2). The lowest values of the H1 shielding are for $\phi \approx \pm 120°$, when either of the lone pairs of the glycosidic oxygen (O1) lies in the O1−C1−H1 plane. In the synperiplanar position (more shielded), these lone pairs are eclipsed with the C1−C2 and C1−O5 bonds, respectively. The "hump" at antiperiplanar position corresponds to such an orientation of O1 lone pairs where the O1−C1−H1 plane is bisecting the angle between them. This direct effect of lone pairs on σ_{iso} for H1 can be well understood from Figure 3 where

TABLE 5: LMO Contributions from Some Selected Bonds to σ Principal Components for Anomeric C1 Carbon as a Function of ϕ Torsion Angle

	C1−O1				C1−H1				C1−O5			
ϕ, deg	σ_{11}	σ_{22}	σ_{33}	σ_{iso}	σ_{11}	σ_{22}	σ_{33}	σ_{iso}	σ_{11}	σ_{22}	σ_{33}	σ_{iso}
0	−62.9	−30.8	1.1	−30.9	−18.1	−29.1	−45.0	−30.7	−53.2	−18.9	−17.2	−29.8
30	−67.8	−29.3	1.5	−31.9	−12.1	−33.3	−46.2	−30.5	−49.6	−17.4	−18.3	−28.5
60	−62.7	−18.0	−11.6	−30.8	−7.3	−37.4	−47.9	−29.6	−49.0	−34.1	−3.4	−28.9
90	−54.8	−13.1	−17.9	−28.6	−9.6	−36.8	−42.7	−29.7	−50.7	−40.1	2.5	−29.4
120	−49.7	−15.6	−17.2	−27.5	−0.9	−46.5	−44.1	−30.5	−49.9	−38.4	1.2	−29.0
150	−54.9	−7.6	−22.9	−28.5	5.5	−51.9	−44.8	−30.4	−47.0	−43.8	4.7	−28.7
180	−60.8	−2.9	−25.0	−29.5	3.1	−49.4	−44.0	−30.2	−46.8	−46.2	6.7	−28.8
210	−61.4	−3.4	−22.6	−29.1	0.5	−47.4	−43.7	−30.2	−48.2	−45.4	6.8	−28.9
240	−59.3	−5.8	−20.2	−28.4	−5.1	−43.6	−42.4	−30.4	−50.9	−41.2	4.7	−29.1
270	−55.7	−11.5	−18.1	−28.4	−15.6	−33.8	−42.4	−30.6	−52.8	−36.4	0.2	−29.7
300	−53.3	−23.4	−11.7	−29.5	−34.0	−15.8	−43.4	−31.1	−53.5	−30.4	−7.3	−30.4
330	−58.4	−29.0	−5.0	−30.8	−26.0	−22.3	−44.1	−30.8	−54.4	−24.1	−11.6	−30.0

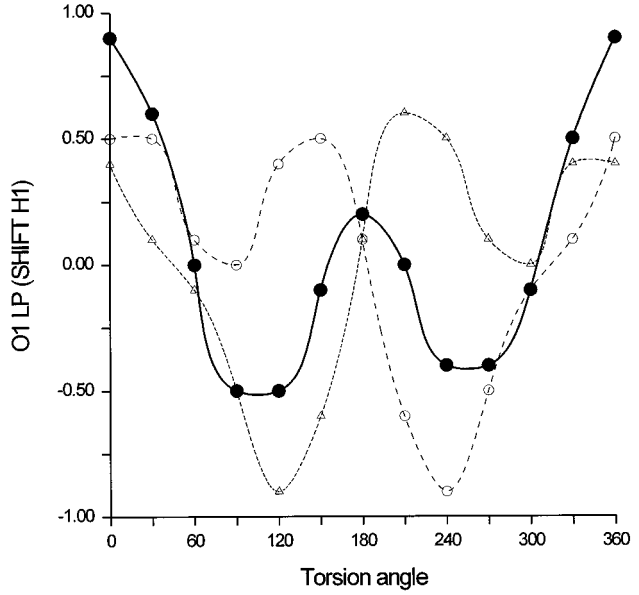

Figure 3. Effect of glycosidic oxygen (O1) lone pairs on H1 chemical shieldings. Dotted and dashed lines depict the effect of LMO contributions from the individual lone pairs (each corresponding to a single lone pair) as a function of the dihedral angle ϕ. The effect is maximal when the lone pair is oriented synperiplanary with respect to the C1−H1 bond; thus, two maxima are shifted by 120°. The solid line shows the sum of both contributions.

the contributions from the O1 lone pairs as functions of ϕ are presented. The maximal deshielding effect (up to 1.4 ppm) is at 120° and 240°, and it is only about 0.5 ppm close to the synperiplanar conformation. It is noteworthy that the overall effect of the lone pairs has nearly the same shape as the total σ_{iso} (Figures 2 and 3). In fact, O1 lone pairs have the dominant influence on H1 shieldings during the conformational changes around the C1−O1 bond. Although the variation in chemical shifts of anomeric proton (up to 0.66 ppm) with the dihedral angle might suggest its usefulness in conformational analysis of oligo- and polysaccharides, the complexity of contributions of other nuclei (mainly protons from the neighboring saccharide units) probably limits such applications. However, in simpler systems, some dependences might be observed experimentally.

Even larger variations of σ_{iso} upon the torsion angle rotation are obtained for ring oxygen (O5) with the range of 18.63 ppm. The highest shielding constant (243.83 ppm) is obtained for ϕ = 120° when O5 and C_{Me} are in the synperiplanar position. In the intervals 0°−30° and 240°−360° O5 shielding remains almost constant (σ_{iso} ∼ 226−229 ppm). A similar trend is observed for the exocyclic oxygen (O1) where the difference between these two ranges of the dihedral angle was somewhat larger (∼30 ppm). A strong dependence of ^{17}O shieldings on the dihedral angle has been observed in 2-alkoxytetrahydropyrans and discussed in terms of anomeric, exo-anomeric, and γ-gauche effects.[37] These effects are closely related to stereoelectronic contributions and changes in geometry within the O5−C1−O1−C_{Me} segment. For example, the γ-gauche effect was attributed to polarization of electrons due to steric interaction[38] as well as changes of geometry (bond lengths and bond angles) "coupled" with torsion changes.[39] Rotation of the OMe group is accompanied (among other geometrical variations) by the changes of the C1−O1−C_{Me} bond angle (Table 3). This bond angle varies from 114° for syn-conformations up to 121° at ϕ = 240° and has an intermediate value (∼117°) for the anti-conformation. To estimate the influence of the magnitude of the C1−O1−C_{Me} bond angle on the shielding constants an additional calculation has been performed. In this case, the C1−O1−C_{Me} bond angle has been changed by 3° (from 116.5° to 119.5°) for the conformation with ϕ = 150°. In the original (optimized) conformation there is a weak internal nonbonded interaction between the methyl proton and the ring oxygen O5 (with the distance of 2.41 Å) which has been removed by increasing the bond angle by 3° (the new distance was 4.71 Å). The resulting variations of σ_{iso} as well as σ_{ii} for both O5 and O1 are, however, only marginal. (σ_{iso} changed from 237.77 to 238.29 ppm and from 271.50 to 271.53 ppm for O5 and O1, respectively.) The changes in shielding tensors for other nuclei were minor as well; e.g., H1 chemical shielding changed by 0.03 ppm. These data support the assumption that variation of the bond angle has nearly negligible influence on chemical shieldings in this molecule and that the observed differences in σ_{iso} are due to stereoelectronic effects. The latter observation agrees with a recent ab initio study in peptide model compounds where the changes in σ_{iso} resulted from torsion angle variations exclusively, without considering any changes in other geometrical parameters that would occur with the dihedral angles variations.[34] However, the influence of geometrical changes upon the magnitudes of chemical shieldings was not negligible in substituted butanes analyzed by the ab initio IGLO method.[40]

3.2. Effect of Torsion on Coupling Constants. Since spin−spin coupling constants depend considerably on the stereochemical arrangement of atoms involved in coupling pathways, there is strong interest to study such dependences. For example, it is well-known that three-bond coupling constants depend on the corresponding dihedral angle (so-called Karplus-type relations),[41] and these dependences have been widely utilized. However, other types of coupling constants, to a smaller or larger extent, vary with dihedral angles as well. For example, the variations of $^1J_{C-H}$ and $^2J_{C-H}$ have been described in various systems as the function of torsion angles,[42,43] and the dependence of $^1J_{C-H}$ has been recently discussed in carbohydrate molecules.[44,45] To analyze such dependencies, the

TABLE 6: Selected Computed One- and Three-Bond Proton−Carbon Coupling Constants (in Hz) as Functions of φ Torsion Angle (deg) in Methyl-β-D-xylopyranoside

	φ, deg											
	0	30	60	90	120	150	180	210	240	270	300	330
$^1J_{C1-H1}$	146.47	149.18	151.20	153.87	156.26	156.20	155.52	158.09	157.63	153.76	148.34	144.95
$^3J_{C(Me)-H1}$	8.29	6.74	3.27	0.17	1.24	5.81	8.23	7.13	2.51	−0.38	1.88	6.25

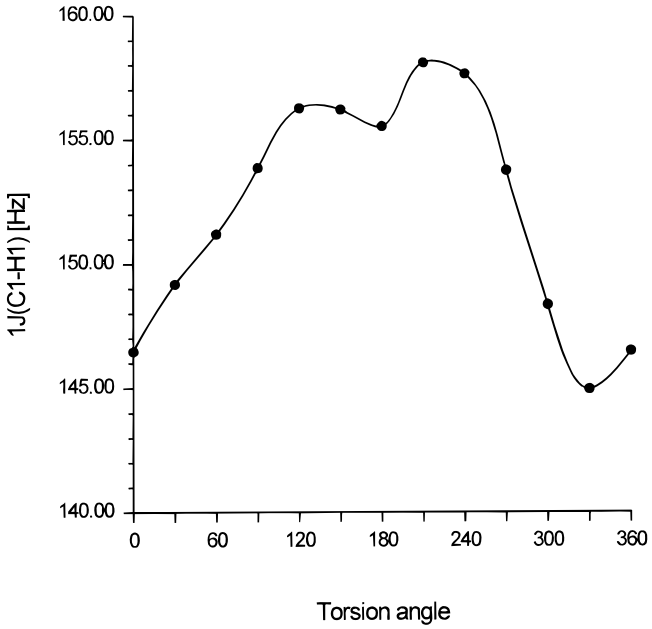

Figure 4. Dependence of the calculated one-bond proton−carbon coupling constant (in Hz) between anomeric carbon (C1) and proton (H1) upon the dihedral angle φ (deg) in methyl-β-D-xylopyranoside.

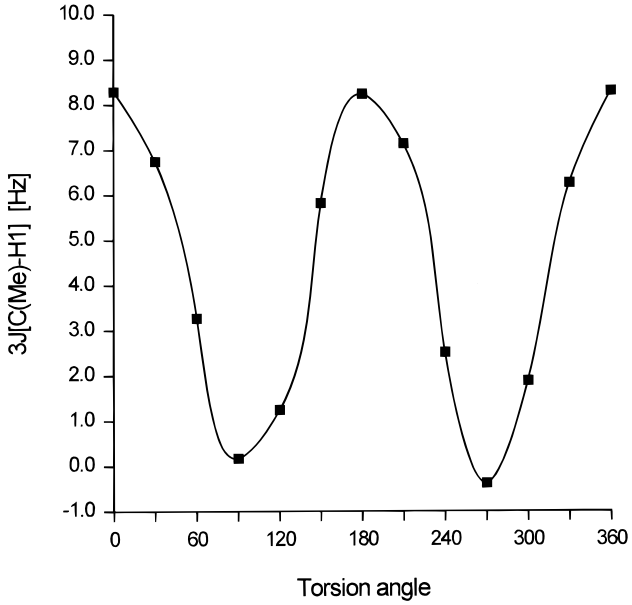

Figure 5. Dependence of the calculated three-bond proton−carbon coupling constants between anomeric proton and methyl carbon ($^3J_{H1-C(Me)}$) upon the dihedral angle φ (deg) in methyl-β-D-xylopyranoside.

calculation of different spin−spin coupling constants for different "relaxed" conformations (described in the previous subsection) in methyl-β-D-xylopyranoside has been performed.

The difference between the computed minimal (at syn-conformation) and maximal (close to anti-conformation) values of $^1J_{C1-H1}$ in methyl-β-D-xylopyranoside is 13.14 Hz (Table 6, Figure 4). This difference is somewhat larger than that in the disaccharide methyl-β-D-xylobioside[44,45] obtained recently by the semiempirical INDO MO method based on crystal structure of the molecule. It seems that in both cases the variations are due to the interaction of O1 electron lone pairs with MO of the C1−H1 bond. As mentioned, this interaction results in the changes not only in geometry (indirect effect) of the whole segment of atoms (as seen for some parameters in Table 3) but also in the electronic structure (direct effect). Both of these effects play an important role in the dependence of $^1J_{C1-H1}$ on the dihedral angle.[46] In particular, the C1−H1 bond length and the C1−O1−C_{Me} bond angle determine this dependence. (However, the behavior of these geometrical parameters is induced by the effects of the O1 and O5 lone pairs.) Two maxima for the values of $^1J_{C1-H1}$ are observed: for conformations close to $\phi = 120°$ and $\phi = 240°$ and, hence, there are some "irregularities" in the bell-shape curve. This type of curve looks similar to the above-discussed dependence of anomeric proton shielding constant (Figure 3). Therefore, this phenomenon has been studied further in a similar way as described in the previous section for O5, O1, and H1 chemical shieldings. Thus, one-bond couplings were computed for both the relaxed and the modified geometries in the C1−O1−C_{Me} array for conformation with $\phi = 150°$. The computed coupling with the modified value of the C1−O1−C_{Me} bond angle (119.5°; increased by 3°) is 157.71 Hz, compared to 156.20 Hz found for the optimized bond angle (116.5°) and thus smoothes the "irregularities"in the $^1J_{C1-H1}$ dependence on φ. The above data clearly demonstrate that the dependence of $^1J_{C-H}$ on φ is directly connected with closely related effects, geometrical changes and stereoelectronic effects, both brought about by O1 (and O5) lone pairs. This observation contrasts to the almost constant values of shieldings found for the same variations of geometry and reflects different dependences of J and σ values on the geometrical parameters in the molecule.

Values of three-bond proton−carbon couplings, $^3J_{H1-C(Me)}$, are listed in Table 6. Their magnitudes change significantly with the torsion angle[41] with the difference between minimum and maximum of about 8.3 Hz. Similarly to $^1J_{C1-H1}$, a slight asymmetry of the curve is observed for this coupling as well (Figure 5). In this case, however, the effect of the torsion angle variation upon $^3J_{H1-C(Me)}$ values seems more complex. Thus, the computed couplings, for the conformation with $\phi = 150°$, with the relaxed and the modified geometry (C1−O1−C_{Me} are 116.5° and 119.5°, respectively) are 5.81 and 6.08 Hz, respectively, and some asymmetry still remains. (For a symmetrical dependence this value should be of about 7 Hz.) It therefore appears that influences of the other atoms are more important, particularly the effect of O5 electron lone pairs. However, more detailed analysis has not been carried out and will be the subject of further studies. It is interesting to note that the magnitudes of $^3J_{H1-C(Me)}$ at syn- and anti-positions are comparable (Figure 5), whereas for the experimentally determined (based on different structures) dependences, three-bond couplings are 1.2 Hz lower for synclinal conformation than those for antiperiplanar conformation.[47,48] This discrepancy is probably due to several factors such as the difference in the structure of compounds, possible effects of packing in the solid state (the calculations have been carried out for an isolated molecule and therefore intermolecular interactions have been neglected), and the errors

caused by the used computational method. However, judging by our experience, we believe that latter are less than 10% for these types of couplings.

4. Conclusions

The computed shielding tensors, proton−proton and proton−carbon spin−spin couplings in monosaccharide methyl-β-D-xylopyranoside calculated with density functional theory (DFT), are in very good agreement with experimental data. The effect of torsion around the glycosidic C1−O1 bond is significant for both σ and J values. Chemical shifts of all nuclei in the acetal segment (^{1}H, ^{13}C, and ^{17}O) depend on the dihedral angle ϕ and indicate that these variations might be potentially useful as conformational probes at the glycosidic linkage. Furthermore, the sensitivity of the σ_{ii} components to variation of the dihedral angle ϕ depends strongly on their spatial orientation as a consequence of the contributions from individual chemical bonds. σ_{iso} is almost independent of the C1−O1−C_{Me} bond angle whereas the spin−spin couplings depend on changes in all geometrical parameters. The variations of $^1J_{C-H}$ in this monosaccharide were found to be larger than those obtained previously in disaccharides. Rather surprisingly, even a simple molecular mechanics (MM2) method yields optimized geometry which is sufficient for reliable DFT calculation of spin−spin couplings.

Acknowledgment. This work was supported by the Slovak Grant Agency VEGA (Grants 2/1235/96 and 2/3008/97). M.H. thanks his colleagues at Institute "G.Ronzoni", Milan, for the access to Bruker AMX 500 spectrometer where a part of NMR experiments was carried out. This work also benefited from the earlier Alexander von Humboldt Fellowship of V.G.M. at the Ruhr University of Bochum, Germany. V.G.M. thanks the Alexander von Humboldt Foundation for donation of an HP9000/C160 workstation used in the present study.

References and Notes

(1) Malkin, V. G.; Malkina, O. L.; Salahub, D. R. *Chem. Phys. Lett.* **1994**, *221*, 91.

(2) Malkin, V. G.; Malkina, O. L; Casida, M. E.; Salahub, D. R. *J. Am. Chem. Soc.* **1994**, *116*, 5898.

(3) Malkin, V. G.; Malkina, O. L.; Eriksson, L. A.; Salahub, D. R. in *Modern Density Functional Theory*: *A Tool for Chemistry*; Theoretical and Computational Chemistry Vol. 2; Seminario, J. M., Politzer, P., Eds.; Elsevier: Amsterdam, 1995.

(4) Grant, D. M.; Facelli, J. C.; Alderman, D. W.; Sherwood, M. H. In *Nuclear Magnetic Shieldings and Molecular Structure*; Tossell, J. A., Ed.; Kluwer Academic Publishers: Dordrecht, 1993; p 367.

(5) Barfield, M. In *Nuclear Magnetic Shieldings and Molecular Structure*; Tossell, J. A., Ed.; Kluwer Academic Publishers: Dordrecht, 1993; p 523.

(6) Liu, F.; Phung, C.; Alderman, D. W.; Grant, D. M. *J. Magn. Reson*. **1996**, *A120*, 231.

(7) Malkina, O. L.; Salahub, D. R; Malkin, V. G. *J. Chem. Phys*. **1996**, *105*, 8793.

(8) Malkin, V. G.; Malkina, O. L.; Steinebrunner, G.; Huber, H. *Chem. Eur. J.* **1996**, *2*, 452.

(9) Malkin, V. G.; Malkina, O. L.; Salahub, D. R. *J. Am. Chem. Soc*. **1995**, *117*, 3294.

(10) Kaupp, M.; Malkin, V. G.; Malkina, O. L.; Salahub, D. R. *Chem. Eur. J.* **1996**, *2*, 24.

(11) Salahub, D. R.; Fournier, F.; Mlynarski, P.; Papai, I.; St-Amant, A.; Ushio, J. In *Density Functional Methods in Chemistry*; Labanowski, J. K., Andzelm, J. W., Eds.; Springer: New York, 1991; p 77.

(12) St-Amant, A.; Salahub D. R. *Chem. Phys. Lett.* **1990**, *169*, 387.

(13) Perdew, J. P. Wang, Y. *Phys. Rev.* **1986**, *B33*, 8800.

(14) Perdew, J. P. *Phys. Rev*. **1986**, *B33*, 8822; **1986**, *34*, 7406.

(15) Perdew, J. P.; Wang, Y. *Phys. Rev*. **1992,** *B45*, 13244.

(16) Becke, A. D. *Phys. Rev*. **1988**, *A38*, 3098.

(17) Kutzelnigg, W.; Fleischer, U.; Schindler, M. In *NMR−Basic Principles and Progress*, Springer-Verlag: Heidelberg, 1990; Vol. 23, p 165.

(18) Godbout, N.; Salahub, D. R.; Andzelm J.; Wimmer, E. *Can. J. Chem*. **1992** *70*, 60.

(19) Daul, C. A.; Goursot, A.; Salahub, D. R. In *NATO ARW Proceedings on Grid Methods in Atomic and Molecular Quantum Calculation*; Cerjan, C., Ed.; Kluwer: Dordrecht, The Netherlands; 1993; Vol. C412.

(20) Mohamadi, F.; Richards, N. G. J.; Guida, W. C.; Liskamp, R.; Lipton, M.; Caufield, C.; Chang, G.; Hendrickson, T.; Still, W. C. *J. Comput. Chem*. **1990**, *11*, 440.

(21) Hricovíni, M.; Tvaroška, I.; Uhrín, D.; Batta, G. *J. Carbohydr. Chem*. **1989**, *8*, 389.

(22) Poppe, L.; Van Halbeek, H. *J. Magn. Reson*. **1991**, *93*, 214.

(23) Taylor, M. G.; Marchessault, R. H.; Pérez, S.; Stephenson, P. J.; Fyfe, C. A. *Can. J. Chem*. **1985**, *63*, 270.

(24) Liu, F.; Phung, C. G.; Alderman, D. W.; Grant, D. M. *J. Am. Chem. Soc*. **1996**, *118*, 10629.

(25) Perlin, A. S.; Casu, B. *Tetrahedron Lett.* **1969**, 2921.

(26) Stahl, M.; Schopfer, U.; Frenking, G.; Hoffmann, R. W. *J. Org. Chem*. **1997**, *62*, 3702.

(27) Saitô, H. *Magn. Reson. Chem*. **1986**, *24*, 835.

(28) Jarvis, M. C. *Carbohydr. Res*. **1994**, *259*, 311.

(29) Hewitt, J. M.; Linder, M.; Pérez, S.; Buleon, A. *Carbohydr. Res*. **1986**, *154*, 1.

(30) Veregin, R. P.; Fyfe, C. A.; Marchessault, R. H.; Taylor, M. G. *Carbohydr. Res*. **1987**, *160*, 41.

(31) Mazeau, K.; Taravel, F. R.; Tvaroška, I. *Chem. Pap*. **1996**, *50*, 77.

(32) Durran, D. M.; Howlin, B. J.; Webb, G. A.; Gidley, M. J. *Carbohydr. Res*. **1995**, *271*, C1.

(33) Kurosu, H.; Ando, I., Webb, G. A. *Magn. Reson. Chem*. **1993**, *31*, 399.

(34) De Dios, A. C.; Oldfield, E. *J. Am. Chem. Soc*. **1994**, *116*, 5307.

(35) Stahl, M.; Schopfer, U.; Frenking, G.; Hoffmann, R. W. *J. Org. Chem*. **1996**, *61*, 8083.

(36) Tvaroška, I.; Bleha, T. *Adv. Carbohydr. Chem. Biochem.* **1989**, *47*, 45.

(37) McKelvey, R. D.; Kawada, Y.; Suguwara, T.; Iwamura, H. *J. Org. Chem*. **1981**, *46*, 4948.

(38) Grant, D. M.; Cheney, B. V. *J. Am. Chem. Soc*. **1967**, *89*, 5315.

(39) Gorenstein, D. G. *J. Am. Chem. Soc*. **1977**, *99*, 2254.

(40) Barfield, M. *J. Am. Chem. Soc*. **1995**, *117*, 2862.

(41) Karplus, M. *J. Chem. Phys.* **1959**, *30*, 11.

(42) Gill, V. M. S.; Von Philipsborn, W. *Magn. Reson. Chem*. **1989**, *27*, 409.

(43) Hansen, P. E. *Prog. NMR Spectrosc.* **1981**, *14*, 175.

(44) Hricovíni, M.; Tvaroška, I. *Magn. Reson. Chem*. **1990**, *28*, 862.

(45) Tvaroška, I.; Taravel, F. J. *J. Biomol. NMR* **1992**, *2*, 421.

(46) Egli, H.; Von Philipsborn, W. *Helv. Chim. Acta* **1981**, *64*, 976.

(47) Tvaroška, I.; Hricovíni, M.; Petrakova, E. *Carbohydr. Res.* **1989**, *189*, 359.

(48) Mulloy, B.; Frenkiel, T. A.; Davis, D. B. *Carbohydr. Res.* **1988**, *188*, 39.